Title
A stress-reduced passaging technique improves the viability of human pluripotent cells

Journal
Cell Reports Methods, 2(2)

ISSN
2667-2375

Authors
Takahashi, Kazutoshi
Okubo, Chikako
Nakamura, Michiko
et al.

Publication Date
2022-02-01

DOI
10.1016/j.crmeth.2021.100155

Peer reviewed

Cell Reports
Methods

Report

A stress-reduced passaging technique improves the viability of human pluripotent cells

Graphical abstract

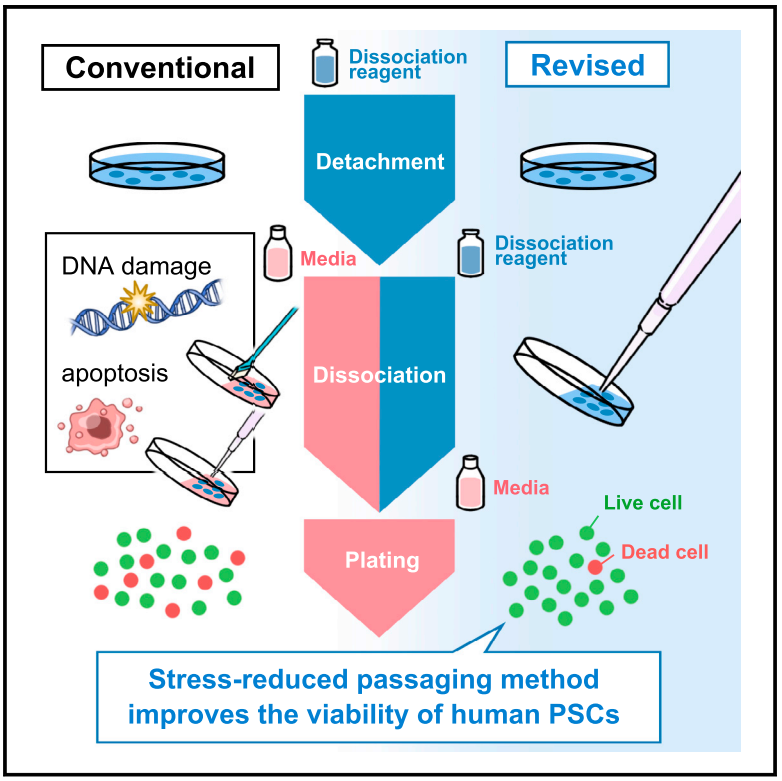

Authors

Kazutoshi Takahashi, Chikako Okubo, Michiko Nakamura, ..., Yousuke Miyamoto, Knut Woltjen, Shinya Yamanaka

Correspondence

kazu@cira.kyoto-u.ac.jp

In brief

Takahashi et al. modify the passaging method for human pluripotent stem cells cultured on recombinant matrices. The revised protocol increases cell viability by reducing DNA damage and apoptosis, improves the efficiency and reproducibility of downstream applications, and attenuates the overgrowth of abnormal cell populations.

Highlights

- An improved passaging method significantly increases the viability of human PSCs
- The method triggers less DNA damage and apoptosis compared to the conventional method
- The stress-reduced method improves the results of downstream applications
- The method attenuates the overgrowth of highly viable abnormal subpopulations

Takahashi et al., 2022, Cell Reports Methods 2, 100155
February 28, 2022
https://doi.org/10.1016/j.crmeth.2021.100155

CellPress

Cell Reports Methods

CellPress
OPEN ACCESS

Report

A stress-reduced passaging technique improves the viability of human pluripotent cells

Kazutoshi Takahashi,[1,4,*] Chikako Okubo,[1] Michiko Nakamura,[1] Mio Iwasaki,[1] Yuka Kawahara,[1] Tsuyoshi Tabata,[1] Yousuke Miyamoto,[1] Knut Woltjen,[1] and Shinya Yamanaka[1,2,3]

[1]Department of Life Science Frontiers, Center for iPS Cell Research and Application, Kyoto University, Kyoto 606-8507, Japan
[2]Gladstone Institute of Cardiovascular Disease, San Francisco, CA 94158, USA
[3]Department of Anatomy, University of California, San Francisco, San Francisco, CA 94143, USA
[4]Lead contact
*Correspondence: kazu@cira.kyoto-u.ac.jp
https://doi.org/10.1016/j.crmeth.2021.100155

MOTIVATION Although chemically defined culture systems for human pluripotent stem cells (PSCs) are in widespread use, cell viability after passaging among PSC clones is often variable, leading to issues with reproducibility. To improve the efficiency and reproducibility of advanced PSC culture systems, we have developed an improved passaging method by optimizing procedures for cell detachment and dissociation. The revised passaging method improves cell viability and makes downstream applications more efficient and reproducible.

SUMMARY

Xeno-free culture systems have expanded the clinical and industrial application of human pluripotent stem cells (PSCs). However, reproducibility issues, often arising from variability during passaging steps, remain. Here, we describe an improved method for the subculture of human PSCs. The revised method significantly enhances the viability of human PSCs by lowering DNA damage and apoptosis, resulting in more efficient and reproducible downstream applications such as gene editing and directed differentiation. Furthermore, the method does not alter PSC characteristics after long-term culture and attenuates the growth advantage of abnormal subpopulations. This robust passaging method minimizes experimental error and reduces the rate of PSCs failing quality control of human PSC research and application.

INTRODUCTION

Xeno-free culture methods for human pluripotent stem cells (PSCs) are widespread. They allow the maintenance of human PSCs, such as embryonic stem cells (ESCs) and induced PSCs (iPSCs), without losing their differentiation potential. The development and optimization of culture vessel-coating reagents, such as synthetic substrates (Melkoumian et al., 2010; Villa-Diaz et al., 2010) and extracellular matrices (Rodin et al., 2010), have contributed to efficient culture systems without the inclusion of animal-derived components, including feeder cells and the Engelbreth-Holm-Swarm mouse tumor-derived basement membrane matrix (i.e., Matrigel) (Thomson et al., 1998; Xu et al., 2001). In particular, recombinant extracellular matrices, such as laminin and vitronectin, allow the rapid and efficient adhesion of undifferentiated PSCs, which express compatible integrin receptors (Chen et al., 2011; Miyazaki et al., 2012; Nakagawa et al., 2014; Rodin et al., 2010; Xu et al., 2001).

Combining such fine-tuned culture systems with inhibitors of cell death, such as the Rho-associated protein kinase (ROCK) inhibitor, dramatically improves the survival of human PSCs during passage and makes the single-cell culture of human PSCs possible (Chen et al., 2021; Watanabe et al., 2007). Furthermore, single-cell cloning following gene disruption or correction by CRISPR/Cas9 facilitates the isolation of PSCs for *in vitro* disease modeling and as possible sources for cell therapies (Hotta and Yamanaka, 2015). In this way, the single-cell culture of human PSCs is a promising method for the systematic quality control of clinical-grade cell lines and reproducibility of basic research.

Unlike advances in the extracellular environment, the passaging procedure has not changed significantly in the last decade. Conventional passaging methods for human PSCs have adhered fundamentally to the classical procedure of dissociating cells after removing/neutralizing the enzymatic activity and/or a chelating reaction by adding growth media (Beers et al., 2012; Chen et al., 2011; Miyazaki et al., 2012; Nakagawa et al., 2014). Considering that the PSC culture conditions have changed significantly, there is room for optimizing the passaging procedure to fit current culture protocols. This study revised a passage protocol for human PSCs cultured in xeno-free

conditions. The method significantly improves the reproducibility of experiments and cell viability. Such controllable passaging facilitated the results of several downstream assays, such as gene editing and differentiation. The modification of the passaging procedure did not change the PSC characteristics, but it did attenuate the growth advantage of abnormal subpopulations. The revised method promises to make PSC cultures safer and further expands the range of human PSC usage.

RESULTS

The conventional method of passaging human PSCs on a xeno-free culture described previously (Figure 1A) (Nakagawa et al., 2014) results in poor reproducibility such as a wide range of cell viability (Figure 1B). To resolve this issue, we modified the procedure of cell passaging and explored the effects on cell viability in detail using two independent iPSC lines (Table S1), WTB6 (Miyaoka et al., 2014) and WTC11 (Kreitzer et al., 2013), maintained on laminin-511 E8 fragment in a chemically defined media, StemFit (Miyazaki et al., 2012; Nakagawa et al., 2014) (Figure 1A). First, we used TrypLE, 5 mM EDTA, or AccuMax (Kim et al., 2016) as the detachment reagent instead of a 1:1 mix of TrypLE and 0.5 mM EDTA (hereafter T1E1), which is used in the conventional method (Miyazaki et al., 2017; Nakagawa et al., 2014). Second, the incubation time was extended from 5 to 10 min. Finally, the dissociation to single cells was performed directly in the detachment solution rather than replacing the detachment solution with growth media and dislodging the cells from the culture vessel using a cell scraper before dissociation. Using this revised method, we could easily detach the cells with all three detachment reagents by gently pipetting up and down. This was nearly impossible with the conventional protocol, which required the use of a cell scraper. As a result of the modifications, the revised method significantly and reproducibly improved the viability of human PSCs (Figures 1B and S1A). In addition to WTB6 and WTC11, the method improved the viability of the iPSC lines such as 201B7 (Takahashi et al., 2007) and 585A1 (Okita et al., 2011) and the ESC line H9 (Thomson et al., 1998) (Table S1) >95% on average (Figure S1B). The revised method also worked well for another xeno-free PSC culture condition combining recombinant vitronectin and Essential 8 media (Chen et al., 2011) (Figure S1C). Since EDTA has been used for the detachment of human PSCs from laminin-511 or vitronectin-coated culture vessels, we tested 5 mM EDTA instead of TrypLE in the revised method (Beers et al., 2012; Chen et al., 2011; Miyazaki et al., 2012). After 10 min of incubation and then dissociation in 5 mM EDTA, the cells were easily detached using a micropipette and showed high viability (Figure 1B). No apparent cytotoxicity was detected in 0.5–5 mM EDTA (Figure S1D), although TrypLE but not EDTA generated single-cell suspensions efficiently by pipetting (Figure S1E). This observation suggests that we can choose TrypLE or EDTA according to the type of downstream assay. These data indicate higher viability of human PSCs in the passaging process.

Next, we systematically tested the detachment and dissociation processes to elucidate which part of the passaging is crucial for viability. We detached human PSCs using TrypLE or T1E1 and then harvested the cells in detachment solution or growth media. We found that the cell viability depended on the condition of the cell dissociation process regardless of the components of the detachment solution (Figure 1C). Using a cell scraper in detachment solution did not decrease the viability, suggesting that damage induced by scraping is not responsible for the cell death in the conventional method (Figure 1D). The data shown in Figures 1C and 1D led us to hypothesize that the enforced cell tearing after replacing the detachment reagent with growth media decreased the cell viability. After replacing the detaching solution with growth media, the cells immediately began to re-attach to the culture vessels, leading to difficult and inefficient cell detachment by pipetting (Figure S1F). Moreover, a longer incubation time in growth media before cell scraping significantly decreased cell viability (Figure 1E). However, prolonged incubation of human PSCs in TrypLE solution did not affect the viability (Figures 1E and S1G). All in all, we concluded that cell dissociation in growth media is a critical step for cell viability.

We found that the revised method not only improves the cell viability immediately after harvesting but also significantly enhances human PSCs' adhesion to the culture vessel upon plating compared to cells collected using the conventional method if the same number of live cells are plated (Figures 1F, 1G, and S1H–S1K). Plating the cells at higher density (1×10^5 cells/cm^2) did not change this tendency (Figure S1L). To quantify the cell adhesion efficiency by eliminating the influence of cell division, we plated the cells at clonal density and counted the number of colonies. As a result, the cells harvested by the revised method formed colonies with 90.2% ± 2.85% adhesion efficiency, whereas those harvested by the conventional method had 51.2% ± 7.34% efficiency, which is similar to a previous report (Figures 1H and S1M) (Miyazaki et al., 2012). Given that plating the same number of live cells just after harvesting by different methods made such a significant difference in the adhesion efficiency, these data suggest that further cell death after plating is a cause of compromised plating efficiency. Antibody-based quantitative protein analysis revealed that a DNA damage marker, phosphorylated Ser139 of histone H2AX variant (γH2AX), and an apoptosis marker, cleaved caspase-3, were significantly increased in cells harvested by the conventional method compared to the revised method (Figures 1I and S2). These data suggest that the revised passaging method improves the viability and adhesion efficiency of human PSCs by not inducing DNA damage or apoptosis.

Based on these results, we thought that such a robust passage could improve the efficiency and accuracy of downstream experiments. We tested whether the revised passaging method increases the yield of clones gene edited by a CRISPR/Cas9 platform. As expected, the cells harvested using the revised method before electroporation generated higher efficiency when targeting the adeno-associated virus integration site 1 (AAVS1) locus than the conventional method (Figure 2A). Next, we examined whether plating an accurate number of cells with high viability facilitates the differentiation of PSCs. Again, as expected, the revised method yielded more troponin T positive cardiomyocytes reproducibly by directed differentiation than cells harvested by the conventional method, which instead caused massive cell death or poor differentiation (Figures 2B and 2C) (Lian et al., 2012). Moreover, the PSCs harvested by

CellPress
OPEN ACCESS

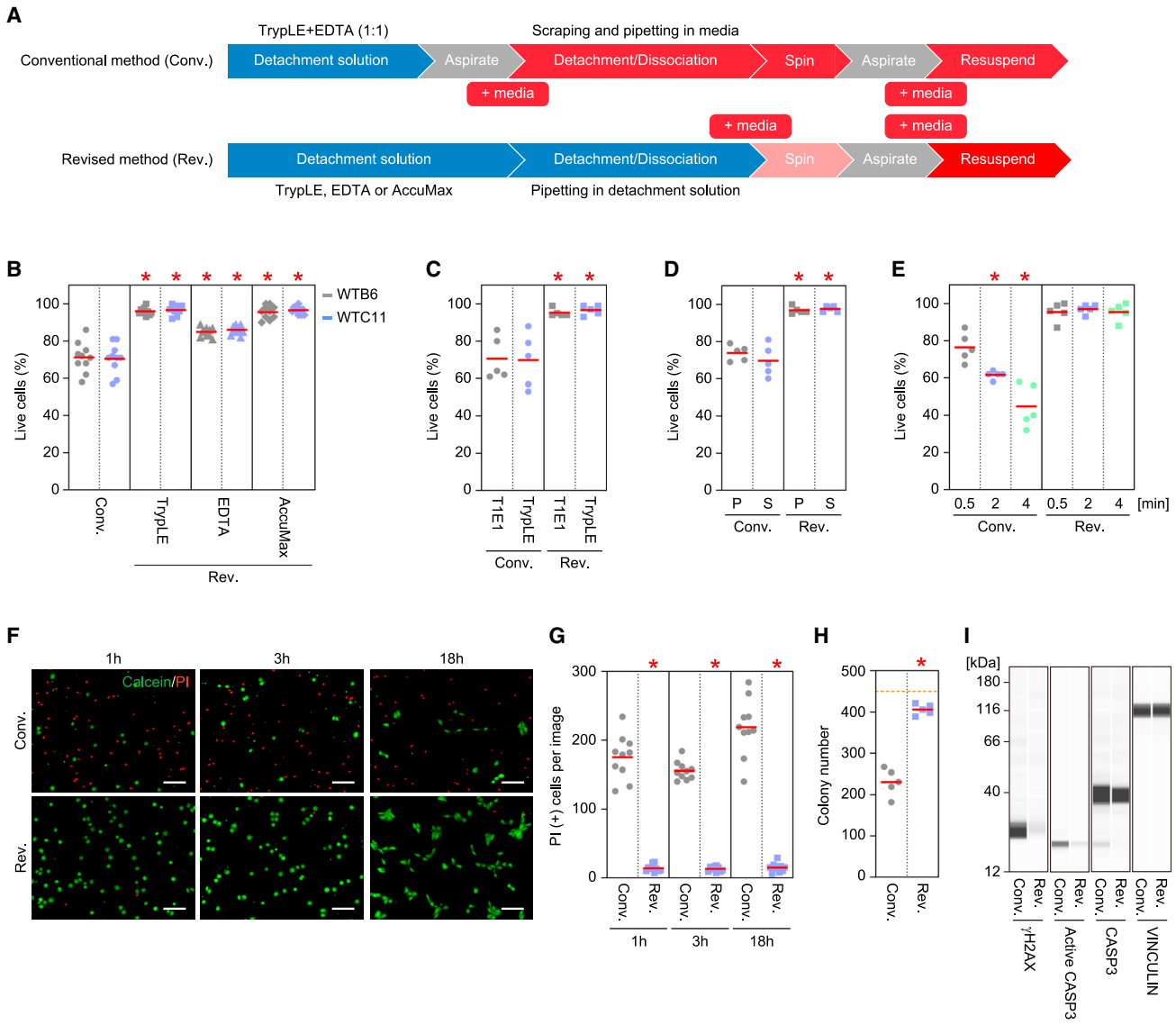

Figure 1. The revised passaging method improves the viability of human PSCs

(A) A flow diagram of the cell passage methods used in the study.

(B) The viability of human PSCs after harvesting using the conventional (Conv.) or revised (Rev.) passaging method. *p < 0.05 versus Conv., one-way ANOVA (Tukey's multiple comparisons test); n = 10.

(C) The viability of human PSCs after harvesting using the Conv. or Rev. passaging method with T1E1 or TrypLE. *p < 0.05 versus Conv., one-way ANOVA (Tukey's multiple comparisons test); n = 5.

(D) The viability of human PSCs after dissociation in growth media (Conv.) or dissociation reagent (Rev.) by pipetting (P) or using a cell scraper (S). *p < 0.05 versus Conv., one-way ANOVA (Tukey's multiple comparisons test); n = 5.

(E) The viability of human PSCs harvested after incubation in dissociation reagent or growth media for the indicated times. *p < 0.05 versus 0.5 min, one-way ANOVA (Tukey's multiple comparisons test); n = 5.

(F) Cell death after plating. Live and dead cells were visualized with calcein (green) and propidium iodide (PI, red), respectively. Bars, 100 μm.

(G) Quantification of dead cells after the indicated times of plating. Ten microscopic views were randomly imaged in each condition and time point, and the number of PI-stained dead cells were counted. *p < 0.05 versus Conv., unpaired t test; n = 10.

(H) The number of colonies derived from PSCs harvested using the Conv. or Rev. method. The mandarin-colored broken line indicates 100% adhesion efficiency. *p < 0.05 versus Conv., unpaired t test; n = 5.

(I) Quantification of DNA damage and cell death marker protein expression. Shown are the virtual blots of phospho-H2AX (γH2AX), cleaved caspase-3 (active CASP3), caspase-3 (CASP3), and VINCULIN in WTB6 iPSCs harvested using the Conv. or Rev. method.

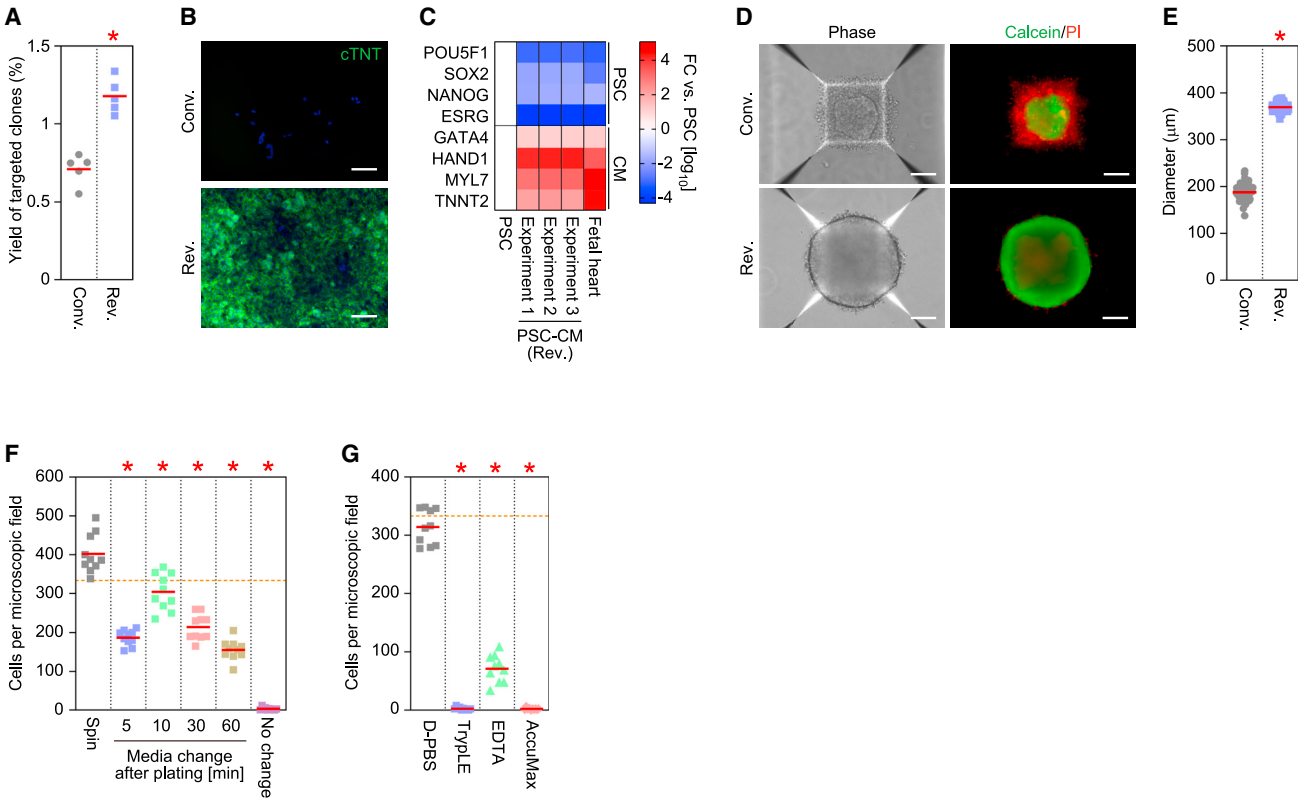

Figure 2. The revised passaging method improves the downstream applications of human PSCs

(A) The yield of AAVS1-targeted colonies. Shown are the number of puromycin-resistant alkaline phosphatase-positive colonies derived from 50,000 iPSCs transfected with the AAVS1 targeting vector and Cas9/sgRNA expression vector. Precisely targeted clones are selected in the presence of puromycin. *$p < 0.05$ versus Conv., unpaired t test; n = 5.

(B) Cardiac differentiation. Representative images of cardiac troponin-T staining (cTNT, green) derived from WTB6 iPSCs are shown. Nuclei were visualized with Hoechst 33342 (blue). Bars, 100 μm.

(C) The quantitative expression analyses of marker gene expression. The heatmap shows relative expressions of the PSC and cardiomyocyte (CM) markers in undifferentiated iPSC, 3 replicates of iPSC-derived CM (PSC-CM) treated with the revised method before the differentiation induction, and fetal heart analyzed by qRT-PCR. Values are normalized by ACTB and compared to iPSC; n = 2. See also Table S2.

(D) Neurosphere formation. Representative images of phase contrast and calcein/PI-stained neurospheres derived from WTB6 iPSCs after 18 h of plating in AggreWell800. Bars, 100 μm.

(E) The diameters of spheres labeled with calcein derived from WTB6 iPSCs harvested using the Conv. (n = 116) or Rev. (n = 114) method were measured. *$p < 0.05$ versus Conv., unpaired t test.

(F) The effects of TrypLE on the adhesion of PSCs. WTB6 iPSCs harvested with the Rev. method were plated in media containing TrypLE. The media was changed at the indicated times after plating or not at all (no change). Microscopic views under a 10× objective were randomly chosen, and the number of nuclei labeled by Hoechst 33,342 were counted. The mandarin-colored broken line indicates 100% adhesion efficiency. *$p < 0.05$ versus Spin., one-way ANOVA (Tukey's multiple comparisons test); n = 10.

(G) The effects of dissociation buffers on the adhesion of PSCs. Cells harvested with the revised method were plated in media containing a 10% volume of D-PBS, TrypLE, 5 mM EDTA, or AccuMax. Microscopic views under a 10× objective were randomly chosen, and the number of nuclei labeled by Hoechst 33342 were counted. The mandarin-colored broken line indicates 100% adhesion efficiency. *$p < 0.05$ versus Spin., one-way ANOVA (Tukey's multiple comparisons test); n = 10.

the revised method efficiently formed neurospheres with few dead cells (Figure 2D) and could produce larger and more uniform-sized spheres than the cells harvested by the conventional method (Figure 2E). These data suggest that the revised passaging method makes downstream applications using human PSCs more efficient and controllable.

Because the revised method dissociates and collects the cells in the detachment reagent, we spun the cells down to remove the supernatant and resuspended the cell pellet in growth media (Figure 1A). The cells suspended in media containing 10% volume of dissociation reagent displayed significantly less adhesion after 18 h of plating, suggesting that removing the detachment reagent is needed (Figures 2F and 2G). Considering our intention to apply the method to automated and/or high-throughput cell culture systems for industrial applications and clinical use, excluding the centrifuge process would be more practical. Therefore, taking advantage of the characteristic that human PSCs rapidly adhere to the culture vessel in the presence of a suitable extracellular matrix, such as laminin-511, we tested whether media containing 10% of the detachment reagent can

CellPress
OPEN ACCESS

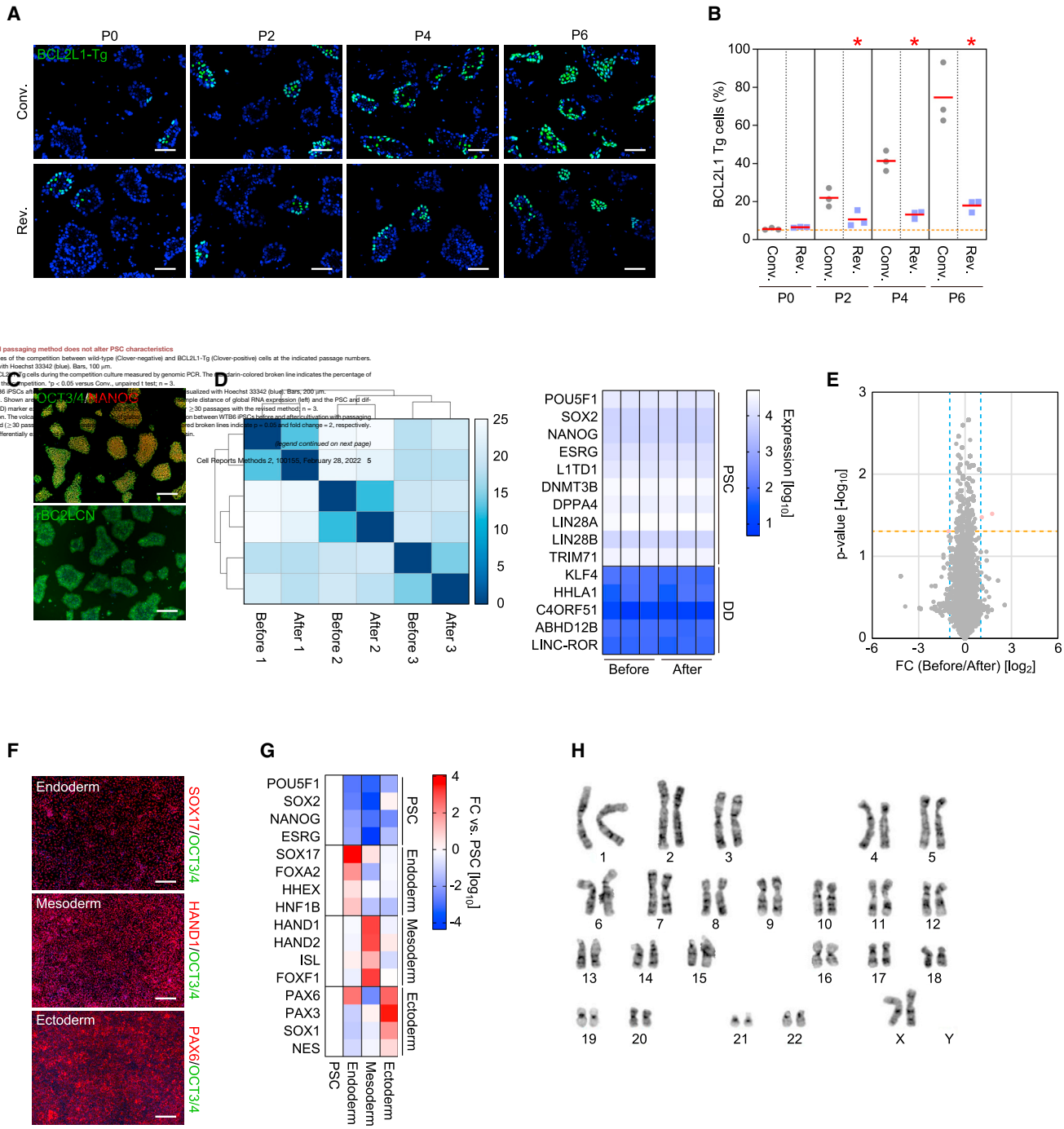

Figure 3. The revised passaging method does not alter PSC characteristics

(A) Representative images of the competition between wild-type (Clover-negative) and BCL2L1-Tg (Clover-positive) cells at the indicated passage numbers. Nuclei were visualized with Hoechst 33342 (blue). Bars, 100 μm.

(B) The percentage of BCL2L1-Tg cells during the competition culture measured by genomic PCR. The [illegible] dashed-colored broken line indicates the percentage of BCL2L1-Tg cells before the competition. *p < 0.05 versus Conv., unpaired t test; n = 3.

(C) PSC markers in WTB6 iPSCs after [illegible] visualized with Hoechst 33342 (blue). Bars, 200 μm.

(D) The RNA expression. Shown are [illegible] ample distance of global RNA expression (left) and the PSC and differentiation-defective (DD) marker e[illegible] ≥ 30 passages with the revised method] n = 3.

(E) The protein expression. The volca[illegible] on between WTB6 iPSCs before and after cultivation with passaging using the revised method (≥ 30 pass[illegible] red broken lines indicate p = 0.05 and fold change = 2, respectively. The red dots indicate differentially e[illegible] ain.

(legend continued on next page)

be replaced with complete growth media after plating. The number of attached cells after 18 h of plating decreased by half by changing the media 5 min after plating (Figure 2F). It is worth noting that changing the media 10 min after plating resulted in a 76.5% ± 14.0% yield based on the number of cells suspended in complete media before plating. The lost quarter of adhered cells is significant, but the result is still much better than the number of adhered cells harvested by the conventional method before plating (Figures 2F and S1I). The revised passaging method is potentially beneficial for the preparation of human PSCs to be used in later applications.

One of the highest priority problems for PSC culture systems is avoiding malignant transformation by the abnormal growth of unexpected subpopulations. Thus, we created a human iPSC line overexpressing BCL2L1, which drives the strong selective advantage of chromosome 20q11.21 amplification (Amps et al., 2011; Avery et al., 2013), and tested the effects of the passage methods on its excessive growth rate. To this end, BCL2L1-transgenic (Tg) iPSCs were added to make up 5% of the total cell number into parental iPSCs and monitored their proportions in co-culture for 6 passages. The revised passaging method significantly attenuated the growth advantage of BCL2L1-Tg iPSCs, whereas the conventional method biased amplification (Figures 3A and 3B). This observation suggests that the revised method keeps human PSCs stable during continuous culture. We validated human PSCs split 30 times over 100 days using the revised method. These cells kept expressing core PSC transcription factors, such as OCT3/4 (Okamoto et al., 1990; Scholer et al., 1990) and NANOG (Chambers et al., 2003; Mitsui et al., 2003), and displayed an affinity for rBC2LCN (Onuma et al., 2013) (Figures 3C and S3A). We confirmed that passaging with the revised method did not induce major changes in global RNA expression, the expression of PSC and differentiation-deficiency (DD) markers (Koyanagi-Aoi et al., 2013; Ohnuki et al., 2014), and global protein expression levels (Figures 3D, 3E, S3B, and S3C). The cells could differentiate into three germ layers through directed differentiation methods (Figures 3F, 3G, S3D, and S3E) and have no apparent karyotype abnormalities (Figures 3H and S3F). These data suggest that the revised passaging method is suitable for human PSC subcultures.

DISCUSSION

In this study, we provide a revised passaging method optimized for the xeno-free culture of human PSCs. The major change compared with the conventional method was cell dissociation before media replacement; other factors such as reagents and mechanical dissociation techniques are flexible. Since human PSCs rapidly adhere to the matrix-coated culture vessel again after replacing dissociation reagent with growth media, forced cell detachment by scraping or pipetting should be stressful (Figures 1I, S1F, and S2). However, we demonstrated that quick cell dissociation after adding growth media achieves relatively better viability (Figure 1E). Although this quick dissociation may be applicable to one-by-one treatment of cultured cells, multi-throughput experiments need a more flexible time window of the dissociation step. Using the revised method, we showed that 10 min of incubation in TrypLE at 37°C for detachment and a subsequent 60 min of incubation at room temperature did not affect the viability of human PSCs (Figure S1G). Therefore, we concluded that the revised method is suitable for the multi- or high-throughput treatment of human PSC cultures.

The continuous commingling of dissociation buffer with the growth media overnight detached human PSCs from the culture vessel, suggesting that dissociation buffer must be removed. The ideal solution for cell viability, then, is replacing the dissociation buffer-containing media with complete media after spinning the cells down. For an automated cell culture system, however, the centrifuging process is preferred to be excluded. We showed a model of the spin-free method by changing the media after plating the cells onto a culture vessel. Removing the dissociation buffer-containing media after 10 min of plating yielded 75% of cells after 18 h of plating compared to spinning the cells down before plating. While there may still be a margin for improvement, this approach is nevertheless an attractive model for PSC-based applications.

The revised passaging method significantly improved downstream applications, in particular, directed differentiation, by improving cell survival and adhesion efficiency. We note that increasing the number of cells plated can improve the results of applications even when using the conventional passaging method, in which reproducibility tends to be low. The use of ROCK inhibitor in the human PSC culture increases the cloning efficiency from <1% to ~25% (Watanabe et al., 2007). In addition, the high affinity between integrin substrates and human PSCs allows for cell viability of ~50% (Beers et al., 2012; Chen et al., 2011; Miyazaki et al., 2012). The stress-reduced passaging method shown in this study combined with the previous findings introduced above enable 90% adhesion efficiency even at clonal density. This study optimized the passaging procedure, which has been relatively ignored compared with the media and matrix in efforts to optimize xeno-free PSC cultures. That improving the passaging method was sufficient to reach a yield with >95% viability suggests that the proper combinations of available xeno-free media and recombinant matrices are already effective for efficient culturing. Since our revised method simply modifies the cell dissociation condition, it can be applied to current procedures without significant modifications and will likely improve the results of basic PSC research and applications.

(F) Directed differentiation of PSCs after ≥30 passages by the revised method into trilineage. Shown are representative immunocytochemistry images of WTB6 iPSC-derived differentiated cells stained for each lineage marker, including SOX17, HAND1, and PAX6 (red), and a PSC marker, OCT3/4 (green). Nuclei were visualized with Hoechst 33342 (blue). Bars, 200 μm.

(G) The expression of lineage markers. The heatmap shows the relative expression of PSC and lineage markers in WTB6-derived directed differentiated cells detected by qRT-PCR. Values are normalized by ACTB and compared to parental iPSC; n = 3. See also Table S2.

(H) A representative G-banding image shows normal 46XX karyotype.

Limitations of the study

The protocol provided in this study is suitable for PSCs maintained on recombinant extracellular matrices that allow for rapid and efficient adhesion. This feature overcomes the issue of forcibly dislodging PSCs after adding growth media, which reduces their viability. The passaging method with the cell dissociation before adding growth media also can be used for classical culture methods that use Matrigel or feeder cells (Ellerström et al., 2007). However, since these culture systems do not have this dislodgement issue, our revised protocol has few advantages. The revised method enhances the viability of cells only during passaging and is less effective during growth (Figures S1J and S1K). Adding cell death inhibitors is still needed to improve the expansion efficiency (Chen et al., 2021; Watanabe et al., 2007).

The present study demonstrated that the revised passaging method could attenuate the growth advantage of a BCL2L1-Tg subpopulation (Figures 3A and 3B). Previous studies showed that chromosome 20 copy number increases including BCL2L1 enhance the viability of human PSCs rather than alter proliferation (Amps et al., 2011; Avery et al., 2013). However, other common karyotypic abnormalities involving the copy-number increases of chromosomes 1, 12, and 17 promote the proliferation of human PSCs (Price et al., 2021). Further studies are needed to demonstrate whether the revised passaging method is effective for such abnormal subpopulations displaying excessive proliferation.

Finally, dissociation with EDTA led to lower viability than TrypLE or AccuMax (Figures 1B, S1C, and S1D). However, as shown in Figure S1E, EDTA treatment did not produce single cells efficiently. Thus, cell viability can be underestimated because of selective single-cell counting. Therefore, we cannot conclude that there is an advantage of enzymatic treatment compared to EDTA.

STAR★METHODS

Detailed methods are provided in the online version of this paper and include the following:

- KEY RESOURCES TABLE
- RESOURCE AVAILABILITY
  - Lead contact
  - Materials availability
  - Data and code availability
- EXPERIMENTAL MODEL AND SUBJECT DETAILS
- METHOD DETAILS
  - Cell culture
  - The revised passaging method
  - Conventional passaging
  - Cell adhesion test
  - Single cell plating in clonal density
  - Live and dead cell staining
  - RNA isolation and quantitative reverse transcription polymerase chain reaction (qPCR)
  - Antibody-based quantitative protein analysis
  - Gene targeting
  - Plasmid construction
  - Generation of BCL2L1-expressing iPSC line
  - Cell competition assay
  - Genomic PCR for copy number quantification
  - Endoderm differentiation
  - Mesoderm differentiation
  - Ectoderm differentiation
  - Cardiomyocyte differentiation
  - Neurosphere formation
  - Immunocytochemistry
  - rBC2LCN staining
  - RNA sequencing (RNA-seq) and data analysis
  - Global proteome analysis
- QUANTIFICATION AND STATISTICAL ANALYSIS

SUPPLEMENTAL INFORMATION

Supplemental information can be found online at https://doi.org/10.1016/j.crmeth.2021.100155.

ACKNOWLEDGMENTS

We thank B. Conklin and K. Okita for sharing materials; K. Higashi, K. Kamegawa, R. Kato, M. Saito, and S. Takeshima for administrative support; M. Ouchida for the graphical abstract; and P. Karagiannis and T. Matsumoto for reading the manuscript. This work was supported by Grants-in-Aid for Scientific Research (20K20585 and 21H02155) from the Japanese Society for the Promotion of Science (JSPS); a grant from the Core Center for iPS Cell Research (JP21bm0104001), the Research Center Network for Realization of Regenerative Medicine from Japan Agency for Medical Research and Development (AMED); a grant from the Takeda Science Foundation; and the iPS Cell Research Fund from the Center for iPS Cell Research and Application, Kyoto University.

AUTHOR CONTRIBUTIONS

Conceptualization, K.T., K.W., and S.Y.; methodology, K.T. and K.W.; investigation, K.T., C.O., M.N., M.I., Y.K., and Y.M.; formal analysis, K.T., C.O., M.I., and T.T.; writing, K.T., C.O., M.I., K.W., and S.Y.; supervision, K.T. and S.Y.

DECLARATION OF INTERESTS

K.T. is on the scientific advisory board of I Peace without salary, M.I. is a scientific adviser for xFOREST Therapeutics without salary, and S.Y. is a scientific advisor for iPS Academia Japan without salary. All of the other authors declare no competing interests.

Received: October 8, 2021
Revised: December 13, 2021
Accepted: December 23, 2021
Published: January 24, 2022

REFERENCES

Amps, K., Andrews, P.W., Anyfantis, G., Armstrong, L., Avery, S., Baharvand, H., Baker, J., Baker, D., Munoz, M.B., Beil, S., et al. (2011). Screening ethnically diverse human embryonic stem cells identifies a chromosome 20 minimal amplicon conferring growth advantage. Nat. Biotechnol *29*, 1132–1144.

Anders, S., Pyl, P.T., and Huber, W. (2015). HTSeq–a Python framework to work with high-throughput sequencing data. Bioinformatics (Oxford, England) *31*, 166–169.

Avery, S., Hirst, A.J., Baker, D., Lim, C.Y., Alagaratnam, S., Skotheim, R.I., Lothe, R.A., Pera, M.F., Colman, A., Robson, P., et al. (2013). BCL-XL mediates the strong selective advantage of a 20q11.21 amplification commonly found in human embryonic stem cell cultures. Stem Cell Rep. *1*, 379–386.

Beers, J., Gulbranson, D.R., George, N., Siniscalchi, L.I., Jones, J., Thomson, J.A., and Chen, G. (2012). Passaging and colony expansion of human pluripotent stem cells by enzyme-free dissociation in chemically defined culture conditions. Nat. Protoc. *7*, 2029–2040.

Chambers, I., Colby, D., Robertson, M., Nichols, J., Lee, S., Tweedie, S., and Smith, A. (2003). Functional expression cloning of nanog, a pluripotency sustaining factor in embryonic stem cells. Cell *113*, 643–655.

Chambers, S.M., Fasano1, C.A., Papapetrou, E.P., Tomishima, M., Sadelain, M., and Studer, L. (2009). Highly efficient neural conversion of human ES and iPS cells by dual inhibition of SMAD signaling. Nat. Biotechnol. *27*, 275–280.

Chen, G., Gulbranson, D.R., Hou, Z., Bolin, J.M., Ruotti, V., Probasco, M.D., Smuga-Otto, K., Howden, S.E., Diol, N.R., Propson, N.E., et al. (2011). Chemically defined conditions for human iPSC derivation and culture. Nat. Methods *8*, 424–429.

Chen, Y., Tristan, C.A., Chen, L., Jovanovic, V.M., Malley, C., Chu, P.H., Ryu, S., Deng, T., Ormanoglu, P., Tao, D., et al. (2021). A versatile polypharmacology platform promotes cytoprotection and viability of human pluripotent and differentiated cells. Nat. Methods *18*, 528–541.

Demichev, V., Messner, C.B., Vernardis, S.I., Lilley, K.S., and Ralser, M. (2020). DIA-NN: neural networks and interference correction enable deep proteome coverage in high throughput. Nat. Methods *17*, 41–44.

Dobin, A., Davis, C.A., Schlesinger, F., Drenkow, J., Zaleski, C., Jha, S., Batut, P., Chaisson, M., and Gingeras, T.R. (2013). STAR: ultrafast universal RNA-seq aligner. Bioinformatics (Oxford, England) *29*, 15–21.

Doi, D., Samata, B., Katsukawa, M., Kikuchi, T., Morizane, A., Ono, Y., Sekiguchi, K., Nakagawa, M., Parmar, M., and Takahashi, J. (2014). Isolation of human induced pluripotent stem cell-derived dopaminergic progenitors by cell sorting for successful transplantation. Stem Cell Rep. *2*, 337–350.

Ellerström, C., Strehl, R., Noaksson, K., Hyllner, J., and Semb, H. (2007). Facilitated expansion of human embryonic stem cells by single-cell enzymatic dissociation. Stem Cells (Dayton, Ohio) *25*, 1690–1696.

Frankish, A., Diekhans, M., Ferreira, A.M., Johnson, R., Jungreis, I., Loveland, J., Mudge, J.M., Sisu, C., Wright, J., Armstrong, J., et al. (2019). GENCODE reference annotation for the human and mouse genomes. Nucleic Acids Res. *47*, D766–D773.

Hotta, A., and Yamanaka, S. (2015). From genomics to gene therapy: induced pluripotent stem cells meet genome editing. Annu. Rev. Genet. *49*, 47–70.

Iwasaki, M., Tabata, T., Kawahara, Y., Ishihama, Y., and Nakagawa, M. (2019). Removal of interference MS/MS spectra for accurate quantification in isobaric tag-based proteomics. J. Proteome Res. *18*, 2535–2544.

Kim, S.I., Oceguera-Yanez, F., Sakurai, C., Nakagawa, M., Yamanaka, S., and Woltjen, K. (2016). Inducible transgene expression in human iPS cells using versatile all-in-one piggyBac transposons. Methods Mol. Biol. (Clifton, NJ) *1357*, 111–131.

Koyanagi-Aoi, M., Ohnuki, M., Takahashi, K., Okita, K., Noma, H., Sawamura, Y., Teramoto, I., Narita, M., Sato, Y., Ichisaka, T., et al. (2013). Differentiation-defective phenotypes revealed by large-scale analyses of human pluripotent stem cells. Proc. Natl. Acad. Sci. U S A *110*, 20569–20574.

Kreitzer, F.R., Salomonis, N., Sheehan, A., Huang, M., Park, J.S., Spindler, M.J., Lizarraga, P., Weiss, W.A., So, P.L., and Conklin, B.R. (2013). A robust method to derive functional neural crest cells from human pluripotent stem cells. Am. J. Stem Cell. *2*, 119–131.

Langmead, B., and Salzberg, S.L. (2012). Fast gapped-read alignment with Bowtie 2. Nat. Methods *9*, 357–359.

Li, H., Handsaker, B., Wysoker, A., Fennell, T., Ruan, J., Homer, N., Marth, G., Abecasis, G., and Durbin, R. (2009). The sequence alignment/map format and SAMtools. Bioinformatics (Oxford, England) *25*, 2078–2079.

Lian, X., Hsiao, C., Wilson, G., Zhu, K., Hazeltine, L.B., Azarin, S.M., Raval, K.K., Zhang, J., Kamp, T.J., and Palecek, S.P. (2012). Robust cardiomyocyte differentiation from human pluripotent stem cells via temporal modulation of canonical Wnt signaling. Proc. Natl. Acad. Sci. U S A *109*, E1848–E1857.

Loh, K.M., Ang, L.T., Zhang, J., Kumar, V., Ang, J., Auyeong, J.Q., Lee, K.L., Choo, S.H., Lim, C.Y., Nichane, M., et al. (2014). Efficient endoderm induction from human pluripotent stem cells by logically directing signals controlling lineage bifurcations. Cell Stem Cell *14*, 237–252.

Loh, K.M., Chen, A., Koh, P.W., Deng, T.Z., Sinha, R., Tsai, J.M., Barkal, A.A., Shen, K.Y., Jain, R., Morganti, R.M., et al. (2016). Mapping the pairwise choices leading from pluripotency to human bone, heart, and other mesoderm cell types. Cell *166*, 451–467.

Love, M.I., Huber, W., and Anders, S. (2014). Moderated estimation of fold change and dispersion for RNA-seq data with DESeq2. Genome Biol. *15*, 550.

Martin, M. (2011). Cutadapt removes adapter sequences from high-throughput sequencing reads. EMBnetjournal *17*, 10–12.

Martin, R.M., Fowler, J.L., Cromer, M.K., Lesch, B.J., Ponce, E., Uchida, N., Nishimura, T., Porteus, M.H., and Loh, K.M. (2020). Improving the safety of human pluripotent stem cell therapies using genome-edited orthogonal safeguards. Nat. Commun. *11*, 2713.

Meier, F., Brunner, A.D., Frank, M., Ha, A., Bludau, I., Voytik, E., Kaspar-Schoenefeld, S., Lubeck, M., Raether, O., Bache, N., et al. (2020). diaPASEF: parallel accumulation-serial fragmentation combined with data-independent acquisition. Nat. Methods *17*, 1229–1236.

Melkoumian, Z., Weber, J.L., Weber, D.M., Fadeev, A.G., Zhou, Y., Dolley-Sonneville, P., Yang, J., Qiu, L., Priest, C.A., Shogbon, C., et al. (2010). Synthetic peptide-acrylate surfaces for long-term self-renewal and cardiomyocyte differentiation of human embryonic stem cells. Nat. Biotechnol. *28*, 606–610.

Mitsui, K., Tokuzawa, Y., Itoh, H., Segawa, K., Murakami, M., Takahashi, K., Maruyama, M., Maeda, M., and Yamanaka, S. (2003). The homeoprotein nanog is required for maintenance of pluripotency in mouse epiblast and ES cells. Cell *113*, 631–642.

Miyaoka, Y., Chan, A.H., Judge, L.M., Yoo, J., Huang, M., Nguyen, T.D., Lizarraga, P.P., So, P.L., and Conklin, B.R. (2014). Isolation of single-base genome-edited human iPS cells without antibiotic selection. Nat. Methods *11*, 291–293.

Miyazaki, T., Futaki, S., Suemori, H., Taniguchi, Y., Yamada, M., Kawasaki, M., Hayashi, M., Kumagai, H., Nakatsuji, N., Sekiguchi, K., et al. (2012). Laminin E8 fragments support efficient adhesion and expansion of dissociated human pluripotent stem cells. Nat. Commun. *3*, 1236.

Miyazaki, T., Isobe, T., Nakatsuji, N., and Suemori, H. (2017). Efficient adhesion culture of human pluripotent stem cells using laminin fragments in an uncoated manner. Sci. Rep. *7*, 41165.

Nakagawa, M., Taniguchi, Y., Senda, S., Takizawa, N., Ichisaka, T., Asano, K., Morizane, A., Doi, D., Takahashi, J., Nishizawa, M., et al. (2014). A novel efficient feeder-free culture system for the derivation of human induced pluripotent stem cells. Sci. Rep. *4*, 3594.

Oceguera-Yanez, F., Kim, S.I., Matsumoto, T., Tan, G.W., Xiang, L., Hatani, T., Kondo, T., Ikeya, M., Yoshida, Y., Inoue, H., et al. (2016). Engineering the AAVS1 locus for consistent and scalable transgene expression in human iPSCs and their differentiated derivatives. Methods (San Diego, Calif) *101*, 43–55.

Ohnuki, M., Tanabe, K., Sutou, K., Teramoto, I., Sawamura, Y., Narita, M., Nakamura, M., Tokunaga, Y., Watanabe, A., Yamanaka, S., et al. (2014). Dynamic regulation of human endogenous retroviruses mediates factor-induced reprogramming and differentiation potential. Proc. Natl. Acad. Sci. U S A *111*, 12426–12431.

Okamoto, K., Okazawa, H., Okuda, A., Sakai, M., Muramatsu, M., and Hamada, H. (1990). A novel octamer binding transcription factor is differentially expressed in mouse embryonic cells. Cell *60*, 461–472.

Okita, K., Matsumura, Y., Sato, Y., Okada, A., Morizane, A., Okamoto, S., Hong, H., Nakagawa, M., Tanabe, K., Tezuka, K., et al. (2011). A more efficient method to generate integration-free human iPS cells. Nat. Methods *8*, 409–412.

Okubo, C., Narita, M., Inagaki, A., Nishikawa, M., Hotta, A., Yamanaka, S., and Yoshida, Y. (2021a). Expression dynamics of HAND1/2 in in vitro human cardiomyocyte differentiation. Stem Cell Rep *16*, 1906–1922.

Okubo, C., Narita, M., Yamamoto, T., and Yoshida, Y. (2021b). RNA-sequencing analysis of differentially expressed genes in human iPSC-derived cardiomyocytes. Methods Mol. Biol. (Clifton, NJ) *2320*, 193–217.

Onuma, Y., Tateno, H., Hirabayashi, J., Ito, Y., and Asashima, M. (2013). rBC2LCN, a new probe for live cell imaging of human pluripotent stem cells. Biochem. Biophys. Res. Commun. *431*, 524–529.

Price, C.J., Stavish, D., Gokhale, P.J., Stevenson, B.A., Sargeant, S., Lacey, J., Rodriguez, T.A., and Barbaric, I. (2021). Genetically variant human pluripotent stem cells selectively eliminate wild-type counterparts through YAP-mediated cell competition. Dev. Cell *56*, 2455–2470.e10.

Rodin, S., Domogatskaya, A., Strom, S., Hansson, E.M., Chien, K.R., Inzunza, J., Hovatta, O., and Tryggvason, K. (2010). Long-term self-renewal of human pluripotent stem cells on human recombinant laminin-511. Nat. Biotechnol. *28*, 611–615.

Scholer, H.R., Dressler, G.R., Balling, R., Rohdewohld, H., and Gruss, P. (1990). Oct-4: a germline-specific transcription factor mapping to the mouse t- complex. EMBO J. *9*, 2185–2195.

Takahashi, K., Tanabe, K., Ohnuki, M., Narita, M., Ichisaka, T., Tomoda, K., and Yamanaka, S. (2007). Induction of pluripotent stem cells from adult human fibroblasts by defined factors. Cell *131*, 861–872.

Takahashi, K., Jeong, D., Wang, S., Narita, M., Jin, X., Iwasaki, M., Perli, S.D., Conklin, B.R., and Yamanaka, S. (2020). Critical roles of translation initiation and RNA uridylation in endogenous retroviral expression and neural differentiation in pluripotent stem cells. Cell Rep. *31*, 107715.

Takahashi, K., Nakamura, M., Okubo, C., Kliesmete, Z., Ohnuki, M., Narita, M., Watanabe, A., Ueda, M., Takashima, Y., Hellmann, I., et al. (2021). The pluripotent stem cell-specific transcript ESRG is dispensable for human pluripotency. PLoS Genet. *17*, e1009587.

Thomson, J.A., Itskovitz-Eldor, J., Shapiro, S.S., Waknitz, M.A., Swiergiel, J.J., Marshall, V.S., and Jones, J.M. (1998). Embryonic stem cell lines derived from human blastocysts. Science *282*, 1145–1147.

Villa-Diaz, L.G., Nandivada, H., Ding, J., Nogueira-de-Souza, N.C., Krebsbach, P.H., O'Shea, K.S., Lahann, J., and Smith, G.D. (2010). Synthetic polymer coatings for long-term growth of human embryonic stem cells. Nat. Biotechnol. *28*, 581–583.

Wang, L., Wang, S., and Li, W. (2012). RSeQC: quality control of RNA-seq experiments. Bioinformatics (Oxford, England) *28*, 2184–2185.

Watanabe, K., Ueno, M., Kamiya, D., Nishiyama, A., Matsumura, M., Wataya, T., Takahashi, J.B., Nishikawa, S., Muguruma, K., and Sasai, Y. (2007). A ROCK inhibitor permits survival of dissociated human embryonic stem cells. Nat. Biotechnol. *25*, 681–686.

Xu, C., Inokuma, M.S., Denham, J., Golds, K., Kundu, P., Gold, J.D., and Carpenter, M.K. (2001). Feeder-free growth of undifferentiated human embryonic stem cells. Nat. Biotechnol. *19*, 971–974.

Young, L., Sung, J., Stacey, G., and Masters, J.R. (2010). Detection of Mycoplasma in cell cultures. Nat. Protoc. *5*, 929–934.

Yusa, K., Zhou, L., Li, M.A., Bradley, A., and Craig, N.L. (2011). A hyperactive piggyBac transposase for mammalian applications. Proc. Natl. Acad. Sci. U S A *108*, 1531–1536.

STAR★METHODS

KEY RESOURCES TABLE

REAGENT or RESOURCE	SOURCE	IDENTIFIER
Antibodies		
Mouse monoclonal anti-OCT3/4	Santa Cruz Biotechnology	Cat# sc-5279, RRID:AB_628051
Goat polyclonal anti-NANOG	R&D Systems	Cat# AF1997, RRID:AB_355097
rBC2LCN-FITC (AiLecS1-FITC)	WAKO	180-02991
Goat polyclonal anti-SOX17	R&D Systems	Cat# AF1924, RRID:AB_355060
Goat polyclonal anti-HAND1	R&D Systems	Cat# AF3168, RRID:AB_2115853
Rabbit polyclonal anti-PAX6	BioLegend	Cat# 901301, RRID:AB_2565003
Mouse monoclonal anti-cardiac Troponin-T	BD Biosciences	Cat# 565744, RRID:AB_2739341
Rabbit monoclonal anti-Phospho-Histone H2A.X (Ser139)	Cell Signaling Technology	Cat# #9718, RRID:AB_2118009
Rabbit monoclonal anti-Cleaved CASPASE-3 (Asp175)	Cell Signaling Technology	Cat# #9664, RRID:AB_2070042
Rabbit polyclonal anti-CASPASE-3	Cell Signaling Technology	Cat# #9662, RRID:AB_331439
Rabbit monoclonal anti-VINCULIN	Cell Signaling Technology	Cat# #13901, RRID:AB_2728768
Alexa 488 Plus donkey anti-mouse IgG	Thermo Fisher Scientific	Cat# A32766, RRID:AB_2762823
Alexa 555 donkey anti-rabbit IgG	Thermo Fisher Scientific	Cat# A31572, RRID:AB_162543
Alexa 647 Plus donkey anti-rabbit IgG	Thermo Fisher Scientific	Cat# A32795, RRID:AB_2762835
Alexa 647 Plus donkey anti-goat IgG	Thermo Fisher Scientific	Cat# A32849, RRID:AB_2762840
Chemicals, peptides, media and recombinant proteins		
iMatrix-511 silk	Nippi	Cat# 892021
Vitronectin (20-398 aa), Human recombinant	WAKO	Cat# 220-02041
StemFit AK02N	Ajinomoto	Cat# AK02
TeSR-E8	Veritas	Cat# ST-05990
Y-27632	WAKO	Cat# 036-24023
Puromycin Dihydrochloride	Thermo Fisher Scientific	Cat# A1113803
Dulbecco's Phosphate Buffered Saline	Nacalai tesque	Cat# 14249-95
UltraPure 0.5 M EDTA, pH8.0	Thermo Fisher Scientific	Cat# 15575020
TrypLE express	Thermo Fisher Scientific	Cat# 12604013
AccuMax	Innovative Cell Technologies	Cat# AM105
STEMdiff SMADi Neural Induction Kit	Veritas	Cat# ST-08581
Activin A, Human recombinant	Nacalai tesque	Cat# 18585-81
BMP4, Human recombinant	Peprotech	Cat# 120-05ET
bFGF, Human recombinant	Peprotech	Cat# 100-18B
PIK-90	Cayman Chemical	Cat# 10010749
PI-103 Hydrochloride	MedChemExpress	Cat# HY-10115A
A83-01	Stemgent	Cat# 04-0014
LDN193189	Stemgent	Cat# 04-0074
CHIR99021	Nacalai tesque	Cat# 18764-44
IWP-4	Stemgent	Cat# 04-0036
DMEM/F-12	Thermo Fisher Scientific	Cat# 10565018
Glasgow's MEM	WAKO	Cat# 078-05525
RPMI1640	Thermo Fisher Scientific	Cat# 11875-093
B27 supplement	Thermo Fisher Scientific	Cat# 17504044
B27 supplement, minus insulin	Thermo Fisher Scientific	Cat# A1895601
Knockout Serum Replacement	Thermo Fisher Scientific	Cat# 10828028
MEM Non-Essential Amino Acids Solution	Thermo Fisher Scientific	Cat# 11140050

(*Continued on next page*)

Continued

REAGENT or RESOURCE	SOURCE	IDENTIFIER
Sodium pyruvate solution	Sigma-Aldrich	Cat# S8636
2-mercaptoethanol	Thermo Fisher Scientific	Cat# 21985023
Critical commercial assays		
Human Stem Cell Nucleofector Kit 1	Lonza	Cat# VAPH-5012
Hoechst 33342	DOJINDO	Cat# H342
Calcein-AM	DOJINDO	Cat# C396
Propidium Iodide	DOJINDO	Cat# P378
BCIP-NBT Solution	Nacalai tesque	Cat# 19880-84
0.4% Trypan blue solution	WAKO	Cat# 207-17081
Fixation buffer	BioLegend	Cat# 420801
4% Paraformaldehyde Solution	Nacalai tesque	Cat# 09154-85
10% TritonX-100 solution	Teknova	Cat# T1105
Normal donkey serum	Sigma-Aldrich	Cat# D9663
QIAzol lysis reagent	QIAGEN	Cat# 79306
miRNeasy Mini Kit	QIAGEN	Cat# 217004
RNase-Free DNase set	QIAGEN	Cat# 79254
DNeasy Blood & Tissue Kit	QIAGEN	Cat# 69504
ReverTra Ace qPCR RT Kit	TOYOBO	Cat# FSQ-101
THUNDERBIRD Next SYBR qPCR Mix	TOYOBO	Cat# QPX-201
TaqMan Universal Master Mix II, no UNG	Thermo Fisher Scientific	Cat# 4440040
TaqMan Assay, human RNase P	Thermo Fisher Scientific	Cat# 4403326
KOD One Master Mix	TOYOBO	Cat# KMM-101
NEBuilder HiFi DNA Assembly Master Mix	New England Biolabs	Cat# E2621
RIPA buffer	Sigma-Aldrich	Cat# R0278
cOmplete Mini EDTA-free Protease Inhibitor Cocktail	Roche	Cat# 4693159001
Pierce BCA Protein Assay Kit	Thermo Fisher Scientific	Cat# 23227
12-230 kDa Jess or Wes Separation Module, 8 x 25 capillary cartridges	proteinsimple	Cat# SM-W004
Anti-Rabbit Detection Module for Jess, Wes, Peggy Sue or Sally Sue	proteinsimple	Cat# DM-001
Agilent RNA6000 Pico Kit	Agilent	Cat# 5067-1513
Agilent High-Sensitivity DNA Kit	Agilent	Cat# 5067-4626
IDT for Illumina RNA UD Indexes Set A, Ligation	Illumina	Cat# 20040553
Illumina Stranded Total RNA Prep, Ligation with Ribo-Zero Plus	Illumina	Cat# 20040529
NextSeq 500/550 High Output v2 Kit	Illumina	Cat# FC-404-2005
SDB-XC Empore disc cartridge	3M	Cat# 2340
Sodium dodecyl sulfate (SDS)	Nacalai Tesque	Cat# 31606-75
Sodium deoxycholate (SDC)	WAKO	Cat# 190-08313
Sodium lauroyl sarcosinate (SLS)	WAKO	Cat# 192-10382
Trypsin / Lys-C Mix, Mass Spec Grade	Promega	Cat# V5072
Ethyl acetate	WAKO	Cat# 051-00356
Acetonitrile	WAKO	Cat# 018-19853
Acetic acid	WAKO	Cat# 018-20061
Formic acid	WAKO	Cat# 066-00461
Trifluoroacetic acid (TFA)	WAKO	Cat# 204-02743
Dithiothreitol (DTT)	WAKO	Cat# 045-08974
Iodoacetamide (IAA)	WAKO	Cat# 095-02151

(*Continued on next page*)

Continued

REAGENT or RESOURCE	SOURCE	IDENTIFIER
Ammonium bicarbonate	WAKO	Cat# 018-21742
1M Tris-HCl (pH 9.0)	Nippon gene	Cat# 314-90381
Protease Inhibitor	Sigma-Aldrich	Cat# P8340
Phosphatase Inhibitor cocktail 2	Sigma-Aldrich	Cat# P5726
Phosphatase Inhibitor cocktail 3	Sigma-Aldrich	Cat# P0044
Aurora column (25 cm length, 75 μm i.d.)	IonOpticks	Cat# AUR25075C18AC
Deposited data		
RNA-seq files	NCBI GEO	GSE184071
Mass spectrometry data files	jPOST	JPST001327 (PXD028731)
Raw images and numerical data	Mendeley	DOI: 10.17632/4c7bvcvj5p.1
Experimental models: Cell lines		
WTB6 human iPSC line	Miyaoka et al. (2014)	RRID:CVCL_VM30
WTC11 human iPSC line	Kreitzer et al. (2013)	RRID:CVCL_Y803
585A1 human iPSC line	Okita et al. (2011)	RRID:CVCL_DQ06
201B7 human iPSC line	Takahashi et al. (2007)	RRID:CVCL_A324
H9 human ESC line	Thomson et al. (1998)	RRID:CVCL_9773
Oligonucleotides		
See Table S2	eurofins, IDT	N/A
Recombinant DNA		
pAAVS1-P-CAG-GFP	Oceguera-Yanez et al. (2016)	Addgene #80491, RRID:Addgene_80491
pXAT2	Oceguera-Yanez et al. (2016)	Addgene #80494, RRID:Addgene_80494
PB-CAG-Clover-P2A-BCL2L1-IP	This study	N/A
Software and algorithms		
Hybrid cell count application BZ-H3C	https://www.keyence.com/global.jsp	KEYENCE
Compass for SW6.0	https://www.proteinsimple.com/compass/downloads/	proteinsimple
STAR Aligner (version 2.5.3a)	https://github.com/alexdobin/STAR	Dobin et al. (2013)
bowtie 2 (version 2.2.5)	http://bowtie-bio.sourceforge.net/bowtie2/index.shtmll	Langmead and Salzberg (2012)
cutadapt-1.12	http://gensoft.pasteur.fr/docs/cutadapt/1.18/index.html	Martin (2011)
SAM tools (version 1.10)	https://sourceforge.net/projects/samtools/files/samtools/1.7/	Li et al. (2009)
RSeQC (version 4.0.0)	http://rseqc.sourceforge.net/	Wang et al. (2012)
HTSeq (version 0.13.5)	https://htseq.readthedocs.io/en/master/	Anders et al. (2015)
DESeq2 (version 1.26.0)	https://bioconductor.org/packages/release/bioc/html/DESeq2.html	Love et al. (2014)
DIA-NN (version 1.8)	https://github.com/vdemichev/DiaNN	Demichev et al. (2020)
Office 365	https://www.office.com/	Microsoft
Adobe Creative Cloud	https://www.adobe.com/	Adobe
GraphPad Prism 8.0.2	https://www.graphpad.com/scientific-software/prism/	GraphPad

RESOURCE AVAILABILITY

Lead contact

Further information and requests for resources and reagents should be directed to and will be fulfilled by the lead contact, Kazutoshi Takahashi (kazu@cira.kyoto-u.ac.jp)

Materials availability

Unique reagents generated in this study are available from the lead contact with a Materials Transfer Agreement.

Data and code availability

- RNA-sequencing and proteome data are accessible in the Gene Expression Omnibus database of the National Center for Biotechnology Information website and in the Japan Proteome Standard Repository/Database, respectively. Accession numbers are listed in the key resources table. The images, numerical data and statical analysis results that were not shown in the paper have been deposited at Mendeley and are publicly available as of the date of publication. The DOI is listed in the key resources table.
- This paper does not report original code.
- Any additional information required to reanalyze the data reported in this paper is available from the lead contact upon request.

EXPERIMENTAL MODEL AND SUBJECT DETAILS

The human pluripotent stem cell (PSC) lines WTB6 iPSC (P49) (RRID:CVCL_VM30), WTC11 iPSC (P46) (RRID:CVCL_Y803), 585A1 iPSC (P49) (RRID:CVCL_DQ06), 201B7 iPSC (P28) (RRID:CVCL_A324), and H9 ESC (P51) (RRID:CVCL_9773) were cultured in humidified incubators at 37°C in 5% CO_2 and 20% O_2. All reagents were warmed in a water bath set at 23°C before use unless otherwise noted. We confirmed all cell lines used in the study were negative for mycoplasma contamination by performing a periodical test (Young et al., 2010). The karyotype analysis was performed by Nihon Gene Research Laboratories, Inc. The experiments using H9 ESCs were conducted in conformity with "The Guidelines on the Distribution and Utilization of Human Embryonic Stem Cells" of the Ministry of Education, Culture, Sports, Science and Technology, Japan. WTB6 and WTC11 were provided by Bruce R. Conklin (The Gladstone Institutes and University of California San Francisco).

METHOD DETAILS

Cell culture

Human PSCs listed in the key resources table were maintained on a laminin 511 E8 fragment (iMatrix, Nippi) in StemFit AK02N media (Ajinomoto) as described previously (Miyazaki et al., 2012; Nakagawa et al., 2014). We also cultured human PSCs on recombinant human vitronectin (20-388 a.a.) (rhVTN, WAKO) in TeSR-E8 media (Veritas) (Beers et al., 2012; Chen et al., 2011). The media was changed daily.

The revised passaging method

In the study, after three days of seeding human PSCs at 2 x 10^5 cells per well of a 6-well plate (~20,000 cells/cm^2), we performed the passaging with the indicated method and reagent unless otherwise stated. The cells were washed once with Dulbecco's Phosphate-Buffered Saline, calcium-free and magnesium-free (hereafter D-PBS, Nacalai tesque) and treated with a dissociating solution, such as TrypLE express (Thermo Fisher Scientific), 0.5-5 mM EDTA, which was prepared by diluting UltraPure 0.5 M EDTA (Thermo Fisher Scientific) in D-PBS, or AccuMax (Innovative Cell Technologies), for 10 min at 37°C. Then the dissociation was performed in the detachment reagent by pipetting up and down using a 1-mL micropipette or using a cell scraper (IWAKI), and the cell suspension was mixed with StemFit AK02N (~10 times volume of dissociation reagent) in a 15-mL tube. Live and dead cells were counted by mixing 1:1 with 0.4% trypan blue solution (WAKO) and using a TC20 automated cell counter (Bio-Rad). After counting the cell number, the cells were spun down at 240 xg for 5 min at room temperature, and the cell pellet was resuspended in StemFit AK02N media. A Rho associate kinase inhibitor, Y-27632 (10 μM, WAKO), and iMatrix (0.25 μg per 1 cm^2 of the culture vessel surface area) were added to the media during the replating (Miyazaki et al., 2017). For the culture system of TeSR-E8 media and rhVTN, the culture vessels were coated with rhVTN (0.75 μg per 1 cm^2) for 1 h at room temperature before use. We routinely plated 2 x 10^5 live cells per well of a 6-well plate and passaged them every three days.

Conventional passaging

The conventional passaging method was described previously (Nakagawa et al., 2014). In brief, the cells were washed with D-PBS and treated with a 1:1 mix of TrypLE express and 0.5 mM EDTA (T1E1) for 5 min at 37°C. Then we aspirated off the supernatant, added an appropriate volume of StemFit AK02N media, harvested the cells using a cell scraper, and collected them in a 15-mL tube. We dislodged the cells using a cell scraper within 30 s after adding the media unless otherwise noted. After that, we counted the cells and plated 2 x 10^5 live cells per well of a 6-well plate in StemFit AK02N media supplemented with 10 μM Y-27632 and iMatrix (0.25 μg per 1 cm^2 of the culture vessel surface area). To fairly compare the two methods, we incubated the cells for 10 min rather than 5 min in TrypLE instead of T1E1 in the experiments shown in the figures except Figures 1B and 1C.

Cell adhesion test

Cells harvested using the indicated dissociation protocol were plated at 2 x 10^5 cells per well of a 6-well plate by the non-coating method (Miyazaki et al., 2017). Eighteen hours after plating, the cells were washed three times with D-PBS and fixed by treating them with 4% paraformaldehyde (BioLegend) for 15 min at room temperature. Then the fixation buffer was replaced with D-PBS supplemented with 1 μg/mL Hoechst 33342 (DOJINDO) and incubated for 60 min at room temperature with protection from light. Ten images of each sample were randomly taken using a BZ-X710 all-in-one fluorescence microscope (KEYENCE), and the number of Hoechst-stained nuclei was counted using a hybrid cell count application BZ-H3C (KEYENCE).

Single cell plating in clonal density

The cells were harvested using the methods indicated above and serially diluted to prepare the cell suspension at 50 live cells/mL in StemFit AK02N plus 10 μM Y-27632 and iMatrix (0.25 μg per 1 cm^2 of the culture vessel surface area). Nine milliliters of the cell suspension containing 450 cells were transferred onto a 100-mm dish and incubated overnight at 37°C. The media was changed every other day with fresh StemFit AK02N. After 8 days of culture, the cells were fixed with 4% paraformaldehyde solution (Nacalai tesque) for 2 min at room temperature and incubated with BCIP-NBT solution (Nacalai tesque) for 60 min to visualize alkaline phosphatase positive colonies.

Live and dead cell staining

The cells were treated with 1 μg/mL of Calcein-AM (DOJINDO) and 2 μg/mL of propidium iodide (PI, DOJINDO) for 15 min at 37°C to discriminate between live and dead cells. After the incubation, the cells were imaged using the BZ-X710 with a 10x objective, and the number of PI positive cells was counted using the BZ-H3C.

RNA isolation and quantitative reverse transcription polymerase chain reaction (qPCR)

The cells were lysed with a QIAzol reagent (QIAGEN), and the total RNA was extracted using a miRNeasy Mini Kit (QIAGEN) with on-column DNase treatment (QIAGEN) according to the manufacturer's protocol. One microgram of purified RNA was applied for the first-strand cDNA synthesis using a ReverTra Ace qPCR RT Master Mix (TOYOBO). Quantitative reverse transcription polymerase chain reaction (qRT-PCR) was performed using a THUNDERBIRD Next SYBR qPCR Mix (TOYOBO) and gene specific primers on a QuantStudio 3 real-time PCR system (Applied Biosystems). The raw Ct values were normalized to the housekeeping gene human ACTB via the double delta Ct method, and then the relative expression was calculated as the fold-change from the control. Primer sequences are listed in Table S2.

Antibody-based quantitative protein analysis

Cells harvested using the conventional or revised method were pelletized by centrifugation and washed once with D-PBS. The pellets were lysed with ice-cold RIPA buffer (Sigma-Aldrich) supplemented with complete EDTA-free protease inhibitor cocktail (Sigma-Aldrich) and stored at −80°C until use. The cell lysates were heated at 95°C for 5 min, spun at 15,300 xg for 15 min at 4°C, and the cleared supernatant was collected and used for the following analysis. The protein concentration was measured using a Pierce BCA Protein Assay Kit (Thermo Fisher Scientific) and EnVision 2104 plate reader (Perkin Elmer) as instructed. We utilized a size-based protein analysis on a Wes automated capillary electrophoresis platform (proteinsimple) and 12-230 kDa Separation Module (proteinsimple) as instructed. We loaded 2.0-2.4 μg of cell lysates for each detection along with the following antibodies: rabbit monoclonal anti-phospho-H2AX (Ser139) (1:25, Cell Signaling Technology), rabbit polyclonal anti-CASPASE-3 (1:50, Cell Signaling Technology), rabbit monoclonal anti-cleaved CASPASE-3 (1:50, Cell Signaling Technology), and rabbit monoclonal anti-VINCULIN (1:250, Cell Signaling Technology). The data was visualized and analyzed using Compass for SW6.0 software (proteinsimple).

Gene targeting

The CRISPR/Cas9-mediated knock-in experiment was performed as described previously (Oceguera-Yanez et al., 2016; Takahashi et al., 2020) with slight modifications. In brief, we transfected 3 μg of pXAT2 and 7 μg of pAAVS1-P-CAG-GFP into 1 million WTB6 iPSCs using a Human Stem Cell Nucleofector Kit I (Lonza) and the A-023 program of a Nucleofector IIb device (Lonza). pXAT2 encodes *S. pyogenes* Cas9 and a single guide RNA (sgRNA) for AAVS1 (5′-GGGGCCACTAGGGACAGGAT-3′). A promoter-less splice acceptor (SA), thosea asigna virus 2A (T2A) peptide and puromycin-resistance gene cassette in pAAVS1-P-CAG-GFP targeting vector is activated by the endogenous AAVS1 promoter only upon correct homologous recombination. Fifty thousand electroporated cells were plated onto a 100-mm dish in StemFit AK02N supplemented with 10 μM Y-27632 and iMatrix (0.25 μg per 1 cm^2 of the culture vessel surface area). Three days after the electroporation, we started the selection with 0.5 μg/mL puromycin and continued it until the non-transfected control died completely and the colonies of the targeted cells grew enough. The colonies were visualized by staining using BCIP-NBT solution, and the number of alkaline phosphatase positive colonies were counted. In this assay, we considered drug-resistant colonies are AAVS1-targeted clones.

Plasmid construction

A triple tandem repeat of Simian Virus 40 nuclear localization signal-tagged Clover (with no stop codon) and a protein coding sequence of human BCL2L1 gene linked in-frame by the porcine teschovirus-derived 2A peptide sequence were generated by

PCR using KOD One Master Mix (TOYOBO). The fragment was inserted into the XhoI site of PB-CAG-IP using NEBuilder HiFi DNA Assembly (New England Biolabs) and verified by sequencing. The resulting plasmid encodes Clover, BCL2L1 and puromycin-resistance gene driven by a constitutively active CAG promoter. The sequence can be provided upon request.

Generation of BCL2L1-expressing iPSC line

We transfected 7 μg of PB-CAG-Clover-P2A-BCL2L1-IP and 3 μg of pCW-hyPBase into one million WTB6 iPSCs as described previously (Takahashi et al., 2020; Yusa et al., 2011). Two days after the transfection, the cells were selected with 0.5 μg/mL of puromycin until the non-transfected cells died completely. The colonies expressing Clover uniformly were chosen and isolated.

Cell competition assay

We added WTB6 iPSCs expressing exogenous BCL2L1 to be 5% of total cell number into parental iPSCs. The mixed cells were plated at 2 x 10^5 cells per well of a 6-well plate and passaged every three days as described above. The cell population was analyzed by the microscopic observation of Clover fluorescence and PCR-based copy number assay for a puromycin-resistance gene.

Genomic PCR for copy number quantification

Genomic DNA was isolated using a DNeasy Blood & Tissue Kit (QIAGEN) according to the manufacturer's protocol. Thirty nanograms of purified DNA was used for qPCR using TaqMan Universal Master Mix II, no UNG (Thermo Fisher Scientific) on a QuantStudio 3 Real Time PCR System. A PrimeTime qPCR Assay (Integrated DNA Technologies) was used to detect the puromycin-resistance gene in the PB-CAG-Clover-P2A-BCL2L1-IP vector, and a TaqMan Copy Number Reference Assay human RNase P (Thermo Fisher Scientific) was used as an internal control. The primer and probe sequences are provided in Table S2.

Endoderm differentiation

The directed differentiation into endoderm was performed as described previously with slight modifications (Loh et al., 2014; Martin et al., 2020). A day before the differentiation, human PSCs were plated at 5 x 10^5 cells per well of a 12-well plate on iMatrix in StemFit AK02N plus 10 μM Y-27632. The cells were treated with 100 ng/mL Activin A (Nacalai tesque), 3 μM CHIR99021 (Nacalai tesque), 20 ng/mL bFGF (Peprotech) and 50 nM PI-103 (Cayman Chemical) in differentiation media 1 (DM1), which consisted of DMEM/F12 (Thermo Fisher Scientific), 2% B27 supplement (Thermo Fisher Scientific), 1% MEM Non-Essential Amino Acids (NEAA, Thermo Fisher Scientific) and 0.1 mM 2-mercaptoethanol (Thermo Fisher Scientific) for 24 h (day 1). Then the cells were cultured in DM1 supplemented with 100 ng/mL Activin A and 250 nM LDN193189 for 48 h (days 2 and 3). Two days later, the cells were maintained in DM1 containing 100 ng/mL Activin A (days 4 and 5). The media was changed daily.

Mesoderm differentiation

Mesoderm differentiation was performed as described previously with slight modifications (Loh et al., 2016; Martin et al., 2020). A day before the differentiation, human PSCs were plated at 5 x 10^5 cells per well of a 12-well plate on iMatrix in StemFit AK02N plus 10 μM Y-27632. The cells were cultured in DM1 supplemented with 30 ng/mL Activin A, 40 ng/mL BMP4 (Peprotech), 6 μM CHIR99021, 20 ng/mL bFGF and 100 nM PIK-90 (MedChemExpress) for 24 h (day 1). Then the cells were cultured in DM1 supplemented with 40 ng/mL BMP4, 1 μM A83-01 and 4 μM CHIR99021 for 48 h (days 2 and 3). Two days later, the cells were maintained in DM1 containing 40 ng/mL BMP4 (days 4 and 5). The media was changed daily.

Ectoderm differentiation

The directed differentiation into neuroectoderm was performed as described previously (Chambers et al., 2009; Doi et al., 2014; Takahashi et al., 2020). A day before the differentiation, human PSCs were plated at 5 x 10^5 cells per well of a 12-well plate on iMatrix in StemFit AK02N plus 10 μM Y-27632. The cells were treated with 1 μM A83-01 and 250 nM LDN193189 in Glasgow's MEM (WAKO) containing 8% Knockout serum replacement (Thermo Fisher Scientific), 1 mM sodium pyruvate (Sigma-Aldrich), 1% NEAA and 0.1 mM 2-mercaptoethanol for 5 days. The media was changed daily.

Cardiomyocyte differentiation

We performed directed cardiomyocyte differentiation as described previously (Lian et al., 2012) with slight modification. Two days before starting the differentiation, cells harvested using the conventional or revised method were plated at 3.5 x 10^5 cells per well of a 12-well plate in StemFit AK02N supplemented with 10 μM Y-27632 and iMatrix (0.25 μg per 1 cm^2 of the culture vessel surface area). On the day we designated as day 0, the media was replaced with RPMI1640 (Thermo Fisher Scientific) supplemented with 2% B27 supplement (minus insulin) and 4 μM CHIR99021. On day 1, we removed CHIR99021. On day 3, we added 5 μM IWP-4 (Stemgent) until day 5. On day 7, we switched the media to RPMI1640 containing B27 supplement (plus insulin) and cultured the cells until day 12.

Neurosphere formation

Cells harvested using the conventional or revised method were transferred at 3 x 10^6 cells per well of an AggreWell 800 24-well plate (Veritas) in STEMdiff Neural Induction Medium supplemented with SMAD inhibitor (Veritas) and 10 μM Y-27632. Then the plate was briefly spun at 100 xg for 3 min and incubated at 37°C for 18 h. After the incubation, we performed Calcein/PI staining as described above. To measure the size of the aggregates, we imaged Calcein positive cells under a 488 nm wavelength filter and measured the diameter of each aggregate using the BZ-H3C. We only evaluated single spheres in a microwell of AggreWell 800 plate.

Immunocytochemistry

Indirect immunocytochemistry was performed as described previously (Takahashi et al., 2021). The cells were washed once with D-PBS and fixed using 4% paraformaldehyde for 15 min at room temperature. The fixed cells were permeabilized and blocked with D-PBS containing 0.1% TritonX-100 (Teknova), 1% bovine serum albumin (BSA, Thermo Fisher Scientific) and 2% normal donkey serum (Sigma-Aldrich) for 45 min at room temperature. We incubated the samples with the primary antibody diluted in D-PBS containing 1% BSA at 4°C for 6-18 h. After washing with D-PBS three times, the samples were incubated with the secondary antibody diluted in D-PBS containing 1% BSA and 1 μg/mL Hoechst 33342 for 45-60 min at room temperature in the dark. After a brief wash with D-PBS, the cells were observed using a BZ-X710. The antibodies used in the study are as follows: mouse monoclonal anti-OCT3/4 (1 μg/mL, SantaCruz), goat polyclonal anti-NANOG (5 μg/mL, R&D systems), goat polyclonal anti-SOX17 (0.5 μg/mL, R&D systems), goat polyclonal anti-HAND1 (5 μg/mL, R&D systems), rabbit polyclonal anti-PAX6 (2 μg/mL, BioLegend), mouse monoclonal anti-cardiac Troponin-T (5 μg/mL, Thermo Fisher Scientific), Alexa 488 Plus donkey anti-mouse IgG (4 μg/mL, Thermo Fisher Scientific), Alexa 555 donkey anti-rabbit IgG (4 μg/mL, Thermo Fisher Scientific), Alexa 647 Plus donkey anti-rabbit IgG (4 μg/mL, Thermo Fisher Scientific) and Alexa 647 Plus donkey anti-goat IgG (4 μg/mL, Thermo Fisher Scientific).

rBC2LCN staining

The cells were washed once with D-PBS and fixed using 4% paraformaldehyde for 15 min at room temperature. The fixed cells were incubated in D-PBS supplemented with 1/100 volume of rBC2LCN-FITC (WAKO) and 1 μg/mL Hoechst 33342 for 30 min at 37°C with protection from light. Then the cells were washed three times with D-PBS and observed using the BZ-X710.

RNA sequencing (RNA-seq) and data analysis

For the RNA-seq analysis, we used WTB6 at early passage (P49, 50 and 51) and late passage (P49+30, 49+31 and 49+32) and WTC11 at early passage (P45, 46 and 47) and late passage (P45+30, 45+31 and 45+32). Cells were lysed using QIAzol reagent, and total RNA was purified as described above. Purified RNA samples were evaluated using an Agilent RNA6000 Pico Kit (Agilent) on a Bioanalyzer 2100 (Agilent). We performed the library preparation and subsequent analysis as described previously (Okubo et al., 2021a, 2021b). In brief, 100 ng of purified RNA was applied to the library construction using the Illumina Stranded Total RNA Prep, Ligation with Ribo-Zero Plus (Illumina). The libraries evaluated using an Agilent High-Sensitivity DNA Kit (Agilent) were sequenced using a NextSeq 500/550 High Output v2 Kit (Illumina). We trimmed the adapter sequence using cutadapt-1.12 (Martin, 2011), excluded reads mapped to ribosomal RNA using SAM tools (version 1.10) and bowtie 2 (version 2.2.5) (Langmead and Salzberg, 2012; Li et al., 2009), aligned the reads to the hg38 human genome using STAR Aligner (Version 2.5.3a) (Dobin et al., 2013; Wang et al., 2012), used RSeQC (version 4.0.0) for the quality check, counted the reads using HTSeq (version 0.13.5) and GENCODE annotation file (version 35) (Anders et al., 2015; Frankish et al., 2019), and normalized the counts using DESeq2 (version 1.26.0) in R (version 3.6.1) (Love et al., 2014). A Wald test was performed using the DESeq2 package.

Global proteome analysis

Cells were lysed with ice-cold PTS lysis buffer consists of 100 mM Tris-HCl, pH9.0 (Nippon Gene), 12 mM sodium deoxycholate (WAKO) and 12 mM sodium lauroyl sarcosinate (WAKO) supplemented with 1% phosphatase inhibitors (Sigma-Aldrich) and 1% protease inhibitor (Sigma-Aldrich). The lysates were subjected to reduction, alkylation, Lys-C/trypsin digestion (enzyme ratio: 1/100) and desalting, as previously described (Iwasaki et al., 2019). Two-hundred and fifty nanograms of the peptides were loaded and separated on an Aurora column (25 cm length, 75 μm i.d., IonOpticks) using a nanoElute (Bruker) for subsequent analysis by timsTOF Pro system (Bruker). The mobile phases were composed of 0.1% formic acid (solution A) and 0.1% formic acid in acetonitrile (solution B). A flow rate of 400 nL/min of 2-17% solution B for 60 min, 17-25% solution B for 30 min, 25-37% solution B for 10 min, 37-80% solution B for 10 min, and 80% solution B for 10 min was used (120 min in total). The applied spray voltage was 1400 V, and the interface heater temperature was 180°C. To obtain MS and MS/MS spectra, the Parallel Accumulation Serial Fragmentation (PASEF) acquisition method with data-independent acquisition (DIA) mode was used (diaPASEF) (Meier et al., 2020). For diaPASEF settings, 1.7 s per one cycle with precursor ion scan and 16 times diaPASEF scans were conducted with the MS/MS isolation width of 25 m/z, precursor ion ranges of 400−1200 m/z, ion mobility ranges of 0.57−1.47 V s cm^2. The obtained DIA data were searched by DIA-NN (v1.8) (Demichev et al., 2020) against selected human entries of UniProt/Swiss-Prot release 2020_03 with the carbamidomethylation of cysteine as the fixed modification and protein N-terminal acetylation and methionine oxidation as the variable modification. For the other DIA-NN parameters, Trypsin/P protease, one missed cleavage, peptide length range of 7-30, precursor m/z range of 300-1800, precursor

charge range of 1-4, fragment ion m/z range of 200-1800, and 1% precursor FDR were used. The values "PG.Normalised" from the results were used as representative protein area values for the comparison.

QUANTIFICATION AND STATISTICAL ANALYSIS

We show the results as individual data (colored dots) and means (red bars) represented by using GraphPad Prism version 8.0.2 (GraphPad). We performed statistical analyses including unpaired, two-tailed t-tests to calculate p-values for the difference between the sample and control using Excel (Microsoft) and one-way analysis of variance (ANOVA) for multiple comparisons (Tukey's multiple comparisons test) using GraphPad Prism 8.0.2. The p-values less than 0.05 were considered significant and are indicated by the asterisks in the figures.